ΣΔ Capacitive Interface for a Vertically-Driven X&Y-Axis Rate Gyroscope

Xuesong Jiang, Sunil A. Bhave, Joseph I. Seeger, Roger T. Howe, Bernhard E. Boser
Berkeley Sensor & Actuator Center
University of California, Berkeley, CA 94720, USA
Email: xsjiang@eecs.berkeley.edu

John Yasaitis
Analog Devices Inc., Cambridge, MA 02139, USA

Abstract

This paper presents the capacitive sensing interface for a vertically-driven X&Y-Axis rate gyroscope fabricated in a monolithic MEMS/circuits technology with 0.8μm CMOS and 6μm thick structural polysilicon. The Coriolis-acceleration transducer and the capacitive sensing interface form a continuous-time 2nd-order 1-bit ΣΔ modulator. The gyroscope achieves 8.6°/sec/√Hz noise floor at atmospheric pressure.

1. Introduction

Gyroscopes find a wide range of applications such as inertial navigation systems, roll-over detection in automobiles and platform stabilization in camcorders and video-game headsets. Micromachined vibratory rate gyroscopes determine rotation rate by vibrating the proof mass and measuring Coriolis acceleration. The axes of detection, vibration and Coriolis acceleration sensing are orthogonal to each other.

X/Y-axis gyroscopes are normally implemented by vibrating the proof mass in a direction parallel to the substrate, either lateral or rotational, and sensing vertical displacement or torsional motion due to Coriolis effect [1, 2].

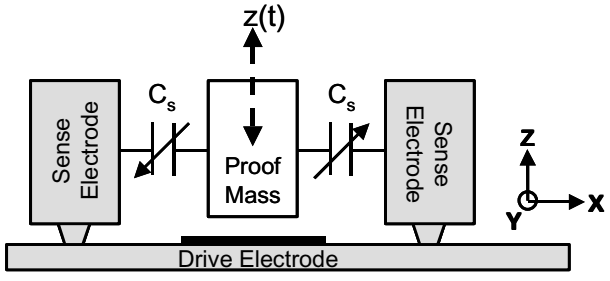

Figure 1. 2D Schematic of vertically-driven Y-axis gyroscope

This paper presents a new X/Y-axis gyroscope based on the principle shown in Figure1. The proof-mass is driven vertically along the Z-axis. Rotation input about the Y-axis generates Coriolis acceleration in-plane along the X-axis. Lateral displacement of the proof mass due to Coriolis acceleration in response to a rotation signal, is detected by a ΣΔ capacitive interface that performs A/D conversion and generates a 1-bit digital output signal. Since a Z-axis gyroscope also detects lateral displacement, all 3-axis gyroscopes can be implemented using a similar capacitive sensing interface. The ΣΔ interface circuit in a Z-axis gyroscope described in [3] has been adapted to implement the capacitive interface for the X&Y-axis gyroscope. The gyroscope is designed to operate at atmospheric pressure with better performance achievable in vacuum. This paper will focus on system modelling and noise issues of the ΣΔ capacitive interface for lateral displacement sensing.

2. Transducer Sensitivity

The transducer of the vertically-driven gyroscope is modelled in Figure 2 as two coupled second-order dynamic systems in orthogonal directions: **drive** (Z-axis) and **sense** (X-axis), which are characterized by masses m_d, m_s, resonant frequencies ω_d, ω_s and quality factors Q_d, Q_s, respectively.

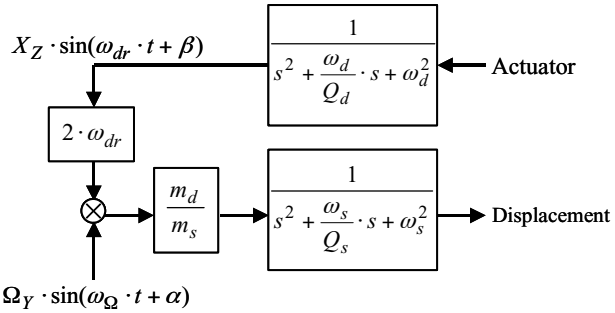

Figure 2. Model of the transducer

The Coriolis acceleration is an amplitude modulated signal with the carrier at the drive frequency ω_{dr}. In response to a sinusoidal rotation rate signal with amplitude Ω_Y, the Coriolis acceleration in a single sideband is given by $\frac{1}{\sqrt{2}} \cdot \frac{m_d}{m_s} \cdot X_Z \cdot \omega_{dr} \cdot \Omega_Y$, where X_Z is the amplitude of the vertical vibration. Large drive amplitude and higher drive frequency helps to increase the Coriolis acceleration. However, it becomes difficult to achieve a large amplitude motion at high frequency

with 5V actuation at atmospheric pressure. In this gyroscope, $m_d / m_s = 0.6$, $\omega_{dr} = \omega_s = 2 \cdot \pi \cdot 16.2kHz$ and $X_Z \approx 200nm$. 1°/sec rotation about the Y-axis corresponds to 15.4μg ($g = 9.8m/s^2$) lateral Coriolis acceleration along the X-axis.

In terms of **sense**, the transducer response to certain Coriolis acceleration is a function of sense resonant frequency ω_s as well as quality factor Q_s if operating near sense resonance. Lower sense resonant frequency is desirable to improve the acceleration sensitivity at the cost of shock resistance. The transducer sensitivity is also affected by Brownian motion noise from the mechanical structure. In this gyroscope with $m_s \approx 2.8\mu gm$ and $Q_s \approx 20$, the Brownian noise floor is 17.6μg/√Hz.

3. ΣΔ closed-loop sensing

ΣΔ closed-loop sensing has been demonstrated in a Z-axis gyroscope [3] and a 3-axis accelerometer [4]. Various noise sources in a ΣΔ closed-loop sensor, e.g. Brownian noise, electronic noise and quantization noise, are normally analysed as independent sources without coupling between each other as in a linear system. However, since the one-bit quantizer is nonlinear, the nonlinear behavior in a ΣΔ modulator [5] needs to be taken into account for the closed-loop noise analysis.

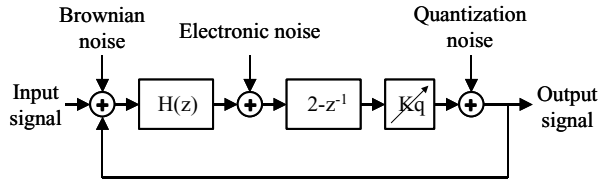

Figure 3. The linear ΣΔ loop model

Figure 3 shows the linear ΣΔ loop model used for noise analysis. $H(z)$ is a discrete-time model for the hybrid ΣΔ sensing system developed based on the method described in [6]. The continuous-time transducer dynamics and the electro-mechanical interface for sensing and force-feedback are modelled in $H(z)$. $2 - z^{-1}$ is the transfer function of the lead filter that ensures the stability of the ΣΔ loop.

The 1-bit quantizer can be modelled as a linear block with a variable gain K_q and an additive noise source as shown in Figure 3. The nonlinearity of the quantizer is accounted for by the variable quantizer gain K_q in this linear model. K_q affects the closed-loop transfer function as well as noise shaping. Once K_q is determined, the resultant linear ΣΔ loop model enables independent noise analysis and superposition of the different noise sources. The linear loop model is effective in noise analysis if the assumption that the input of the quantizer is a Gaussian distributed random signal is satisfied. Simulations are necessary for analysis of stability and tonal behavior of the loop.

The effective quantizer gain K_q is determined by its input variance. In general, the narrow band Coriolis signal has little effect on K_q, hence, we will only consider effects of various noise sources. In an ideal ΣΔ modulator, quantization noise determines K_q. However, in the gyroscope ΣΔ sensing loop, K_q depends on quantization noise as well as Brownian noise and electronic noise. The noise spectrum at the input and the output of the quantizer is shown in Figure 4**.**

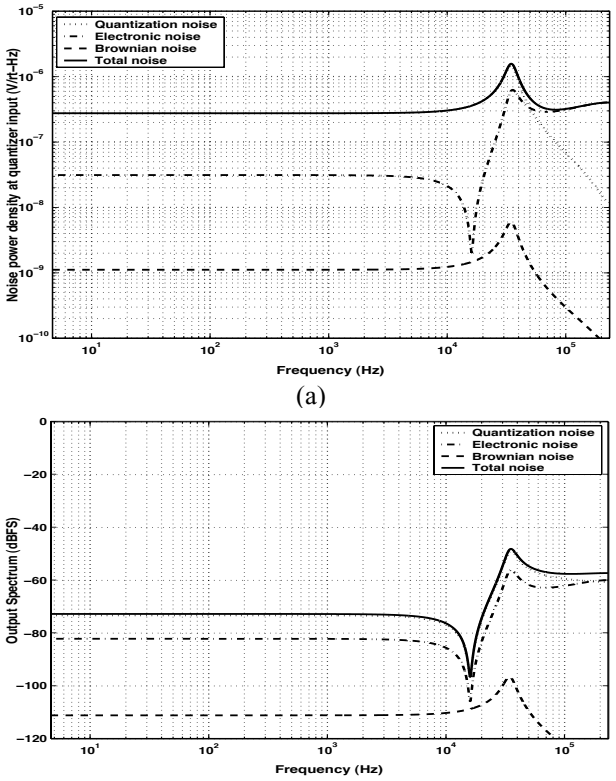

Figure 4. Noise shaping - (a) at quantizer input (b) at quantizer output

Brownian noise and quantization noise have the same noise shaping at the quantizer input. However, at the output of the quantizer, quantization noise in the signal band near the sense resonant frequency is attenuated by the loop-gain. Unless in-band Brownian noise is several orders of magnitude higher than in-band quantization noise, Brownian noise will not affect the quantizer gain and the ΣΔ noise shaping.

The scenario is different for electronic noise. Electronic noise and quantization noise have the similar noise shaping at the quantizer output. However, at the quantizer input, quantization noise passes through the loop filter $H(z)$ and is attenuated at high frequencies, while electronic noise is higher at high frequencies due to noise shaping. Hence at high frequencies electronic noise dominates as shown in Figure 4(a). The quantizer gain

K_q is thus affected by both quantization noise and electronic noise.

It is seen from Figure 3 that Brownian noise is added before the loop filter and electronic noise is added after it. In a standard ΣΔ modulator, the noise from the later stage is attenuated by the gain of the previous stages. However, in the electro-mechanical ΣΔ sensing loop, it is difficult for the mechanical transducer to provide enough gain before the capacitive interface. Without further amplification before the quantizer, the RMS noise at the quantizer input is about 350μV.

It is desirable to design a ΣΔ closed-loop sensor that is dominated by Brownian noise, which fundamentally limits the sensor noise performance. For the gyroscope operating near the sense resonant frequency, the quantization noise can be reduced by either increasing the oversampling ratio of the low-pass ΣΔ modulator that is determined by the sampling frequency and the sense resonant frequency or increasing Q_s. Electronic noise of the capacitive interface, acting as a dither signal in the 2nd-order ΣΔ loop, should not affect the effective quantizer gain K_q significantly.

4. CMOS capacitive interface

The CMOS capacitive interface of the X/Y-axis gyroscope is adapted from that used in a Z-axis gyroscope [3]. The switched-capacitor differential sensing circuit operates with a single 5V supply. In order to improve the sensitivity, the sense voltage is maximized at 5V. Separate capacitors for sensing and force-feedback are designed to prevent higher-order dynamics of the transducer from affecting the ΣΔ loop stability [7]. The nominal sense capacitance is 60fF associated with 300fF parasitic capacitance. The polysilicon wiring resistance from the transducer to the CMOS circuit is 2.7kΩ that adds noise to the capacitive interface.

The feedback capacitance is 80fF and 5V is used for the force-feedback that generates 14g acceleration. The feedback force also compensates linear acceleration along the sensing axis. External linear accelerations are normally at low frequencies. Since the Coriolis acceleration signal is modulated by the drive frequency, linear accelerations do not affect the detection of rotation.

The operation of the sensor in one sampling period T_s is divided into 4 phases: $1/32 \cdot T_s$ reset phase, $1/4 \cdot T_s$ correlated double sampling (CDS) phase, $1/32 \cdot T_s$ evaluation phase for 1-bit A/D conversion and $1/4 \cdot T_s$ feedback phase. The clocks for actuation and sensing are derived from an off-chip master clock. The sampling frequency is $1/32$ of the master clock frequency. The loop delay due to the multi-phase operation has been modelled in the discrete-time loop. In CDS phase, the voltage on the proof mass switches from 5V to 0V. Since the input common mode voltage of the amplifier in the first stage of the capacitive interface is below 5V, the CDS operation contributes additional loop delay to that caused by evaluation phase and feedback phase. Folded cascoded amplifier is used for this first stage. The amplifier has NMOS input transistors and its input common mode voltage is close to 5V in order to reduce loop delay due to the CDS operation.

5. Measurement results

The vertically-driven X&Y-axis gyroscope is implemented in an integrated surface micromachining technology with 0.8μm CMOS electronics and 6μm thick structrual polysilicon. The microphotograph of the X&Y-axis gyroscope is shown in Figure 4.

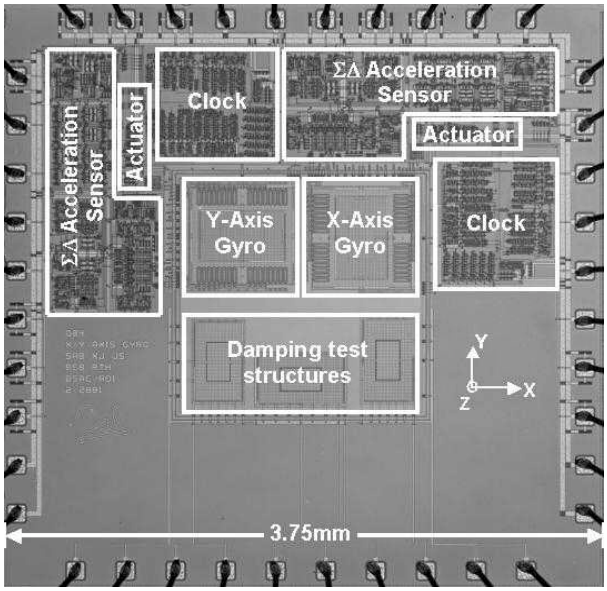

Figure 4. Gyroscope microphotograph

The vertical displacement of the drive mass is characterized using a microvision system [8]. The microvision system measures 370nm peak-to-peak displacement at 16.2kHz at atmospheric pressure.

The 1-bit output bit-stream of the gyroscope is read into a computer and processed using Matlab. The gyroscope is tested on a rate table. Figure 5 shows the output spectrum of the gyroscope in response to a 94°/sec (0-peak) and 2Hz sinusoidal rotation. Since the resonant frequencies of sense and drive are not the same, the drive amplitude at 16.2kHz (i.e. the sense resonant frequency) is only 185nm at atmospheric pressure, which limits the performance to 8.6°/sec/√Hz.

The ΣΔ capacitive interface has been characterized on the shaker table to evaluate its acceleration sensitivity as well as displacement resolution. Figure 6 compares the simulated and measured output noise spectrum of the gyroscope. The off-chip master clock is 15MHz and the sampling frequency is about 470kHz. The signal at 100Hz corresponds to 230mg. The full-scale feedback

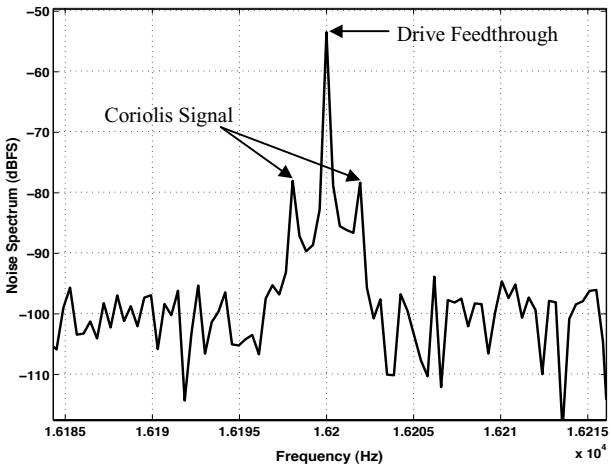

Figure 5. Gyroscope output in response to a 94°/sec (0-peak), 2Hz sinusoidal rate signal

corresponds to 3.4g. The noise floor at low frequencies is 2mg/√Hz and the noise floor at the sense resonant frequency is 115μg/√Hz. The capacitive interface is able to resolve 1.9×10^{-3} nm displacement in 1Hz bandwidth.

Table 1 summarizes the performance of the gyroscope.

Table 1. Performance Summary

Process	0.8μm CMOS 6μm mechanical poly
Mass	1.6μgm (drive) 2.8μgm (sense)
Resonant frequency	13.9kHz (drive) 16.2kHz (sense)
Quality factor	4.2 (drive) 17.6 (sense)
Noise floor	8.6°/sec/√Hz
Displacement resolution	1.9×10^{-3}nm/√Hz

6. Conclusion

We present the ΣΔ capacitive interface for a vertically-driven X&Y axis gyroscope. Various noise sources in the loop are analysed using a linear loop model that takes into account the nonlinear behavior of the ΣΔ modulator. The noise floor of the gyroscope at atmospheric pressure is 8.6°/sec/√Hz.

7. Acknowledgement

The authors like to thank DARPA for funding the project under agreement F30602-97-2-0266.

8. References

[1] T. Juneau, A. P. Pisano, and J. H. Smith, "Dual Axis Operation of a Micromachined Rate Gyroscope", *Transducers 97*, Chicago, June 1997, pp.883-6.

[2] J. Bernstein, S. Cho, A. T. King, A. Kourepenis, P. Maciel, and M. Weinberg, "A Micromachined Comb-Drive Tuning Fork Rate Gyroscope", *Proceedings of IEEE Micro Electro Mechanical Systems*, Fort Lauderdale, February 1993, pp.143-8.

[3] X. Jiang, J. I. Seeger, M. Kraft, and B. E. Boser, "A Monolithic Surface Micromachined Z-Axis Gyroscope with Digital Output", *2000 Symposium on VLSI Circuits*, Hawaii, June 2000, pp. 16-19.

[4] M. Lemkin and B. E. Boser, "A Three-Axis Micromachined Accelerometer with a CMOS Position-Sense Interface and Digital Offset-Trim Electronics", *IEEE Journal of Solid-State Circuits*, Vol.34, April 1999, pp.456-68.

[5] S. H. Ardalan and J. J. Paulos, "An Analysis of Nonlinear Behavior in Delta-Sigma Modulators", *IEEE Transactions on Circuits and Systems*, June 1987, pp.593-603.

[6] O. Shoaei, W. M. Snelgrove, "Design and Implementation of a tunable 40MHz-70MHz Gm-C Bandpass Delta Sigma Modulator", *IEEE Transactions on Circuits and Systems*, Vol. 44, July 1997, pp.521-30.

[7] J. I. Seeger, X. Jiang, M. Kraft, and B. E. Boser, "Sense Finger Dynamics in A Sigma Delta Force-Feedback Gyroscope", *2000 Solid-State Sensor and Actuator Workshop*, Hilton Head Island, June 2000, pp.296-9.

[8] C. Rembe, L. Muller, R. S. Muller, R. T. Howe, "Full Three-Dimensional Motion Characterization of a Gimballed Electrostatic Microactuator", *2001 IEEE International Reliability Physics Symposium*, Orlando, pp. 91-8.

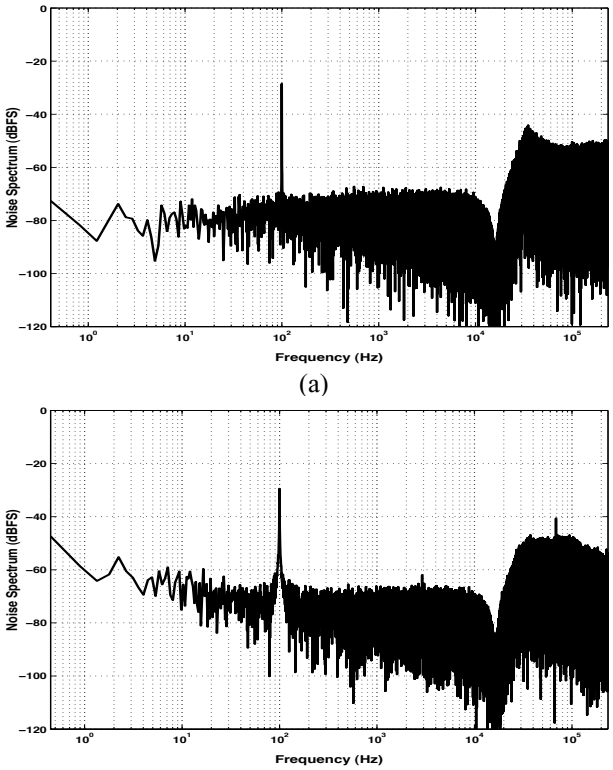

Figure 6. Output noise spectra (a) Simulation (b) Measurement